ELSEVIER

Surface Science 425 (1999) 57–67

surface science

Growth and alloy formation studied by photoelectron spectroscopy and STM

A. Ramstad, F. Strisland [1], S. Raaen *, T. Worren, A. Borg [2], C. Berg

Department of Physics, Norwegian University of Science and Technology (NTNU), Trondheim N-7034, Norway

Received 10 October 1998; accepted for publication 4 January 1999

Abstract

We have grown epitaxial submonolayers of Re on a Pt(111) surface. This system was studied by high-resolution photoelectron spectroscopy and scanning tunneling microscopy (STM). Re was found to grow, at room temperature, as single-layer islands consisting of ~100 atoms. Core-level spectroscopy showed that these islands contain two different species of Re. We interpret these as Re in the centre and on the edges of the islands, where Pt and Re may be intermixed at the edges. Annealing of the Re covered crystal to 1000 K produces a surface alloy with a high degree of local order and a thickness of approximately three layers. The structure of the alloy depends on the Re coverage prior to annealing. Valence band spectra show a strong depletion of Pt 5d states near the Fermi energy when Re is adsorbed, possibly caused by a Pt d→sp rehybridization.

Keywords: Growth; Low-index single crystal surfaces; Metallic films; Platinum; Rhenium; Scanning tunneling microscopy; Synchrotron radiation photoelectron spectroscopy

1. Introduction

The rational design of improved catalysts is one of the major goals of surface science. Altering gas–surface interactions by adding a second metal to the catalyst is one way of improving its performance. In this article, we present a high-resolution photoemission and scanning tunneling microscopy (STM) study of epitaxially grown Re, in the submonolayer regime, on the Pt(111) surface. As well as being of fundamental interest (intermetallic interactions), this system may be viewed as a model for the Pt–Re/Al_2O_3 reforming catalyst. The (111) surface of Pt is chosen because it is the most stable surface and therefore the most common facet on Pt particles.

Re/Pt(111) model systems have been studied by several authors (see, for example, Refs. [7]). Changes in the adsorption rates of small molecules [3] as well as in chemical reaction rates [4,5] have been reported that cannot be described as linear combinations of the corresponding rates for Pt and Re. These authors have suggested that electronic interaction between Pt and Re is responsible for the observed non-linearity. In the following, we will show that there is indeed strong hybridization between Pt and Re, and gain some insight into the details of this interaction. It has also been pointed out [4,6,7] that alloying between Pt and Re alters the catalyst's behaviour. We have studied this phenomenon and found that annealing

* Corresponding author. Fax: +47 73-59-77-10; e-mail: sraaen@phys.ntnu.no.

[1] Present address: SINTEF Electronics and Cybernetics, P.O. Box, 124, Blindern, N-0314 Oslo, Norway.

[2] Present address: Ame Space A/S, N-3189, Norway.

0039-6028/99/$ – see front matter
PII: S0039-6028(99)00185-5

of Re covered surfaces to 1000 K produces a surface alloy with a high degree of local order and even stronger Pt–Re hybridization.

2. Experimental

The photoemission experiments presented in this article were performed at beamline 22 of the MAX I synchrotron radiation source in Lund, Sweden. This beamline is equipped with a large hemispherical electron energy analyzer (Scienta) and a modified Zeiss SX-700 monochromator [8]. The overall resolution in the measurements of the 4f levels of Re and Pt was better than 60 meV. Binding energies were calibrated by measuring the position of the Fermi edge after each spectrum. All spectra were recorded near normal emission, accepting electrons from a cone of $\sim 30^{\circ}$. The Pt crystal was cooled to ~ 100 K during photoemission measurements. The base pressures were $\sim 1 \times 10^{-10}$ Torr in the preparation chamber and $\sim 6 \times 10^{-11}$ Torr in the analysis chamber.

The Pt crystal was cleaned by 2 keV Ar^{+}-sputtering; first at room temperature (RT) in order to remove Re from the surface and to prevent Re diffusion into the bulk, and subsequently at 1100 K. Then annealing was carried out at 1000 K in oxygen at 1×10^{-8} Torr, and finally annealing in vacuum at 1300 K. The crystal was heated by passing a current through the tungsten wire to which it was mounted, and its temperature was monitored by a chromel–alumel thermocouple spot welded to its back. Photoemission spectra of core and valence regions of the most likely contaminants (Re, C, O) showed that this procedure produced a clean Pt surface. A sharp LEED pattern showed that the surface was well ordered.

The STM measurements were performed in the home laboratory using an Omicron UHV STM, equipped with a tungsten tip mounted on a tripod piezoscanner. The images presented in this article are recorded at RT in constant current mode with tunneling parameters as detailed in the figure captions. In the STM laboratory, the cleaning procedure was as described above, except for the use of 1 keV Ar ions. Here, a clean sample was confirmed by a sharp LEED pattern and a high-quality, atomically resolved STM image.

The Pt sample was kept at RT during Re deposition. Re was evaporated from the tip of a Re wire heated by ~ 1 keV electron bombardment. Evaporation was carried out 30 s at a time in order to keep the evaporation rate steady and to maintain a low pressure. During evaporation, the pressure in the chamber rose to $\sim 5 \times 10^{-10}$ Torr. After evaporation, the surface was again routinely tested for C and O contaminations by photoemission. No significant contaminations were found.

3. Results and discussion

3.1. Room-temperature growth

Fig. 1 shows a series of STM images of Re/Pt(111) with Re coverages ranging from 0.25 to 1.0 ML. Each image shows a (different) 1000×1000 Å area consisting of several terraces with Re islands. Typical island radii are between 20 and 30 Å, corresponding to ~ 100 atoms per island. Comparing the height of these islands with that of single atomic steps, we find that they are both 2.0–3.0 Å high. Heights measured by STM are never exact, but we note that they correspond roughly to the heights of single atomic steps on Pt(111) and Re(0001), which are 2.27 and 2.23 Å, respectively. Only the brighter appearing islands in the highest coverage images are thicker than ~ 4 Å. Even at 0.9 ML coverage (Fig. 1d), these cover less than $\sim 5\%$ of the surface, showing that the growth mode is very close to layer-by-layer growth. We have imaged growth at deposition rates ranging from approximately 0.05 to 0.5 ML min^{-1}, always obtaining similar results. In fact, we find no noticeable change in the island size distribution between these deposition rates. Fig. 2 shows a 50×50 Å close-up of a (smaller than average) Re island. In this image, both the island and the substrate are atomically resolved. It is difficult to distinguish between hollow or bridge site adsorption. In fact, we find that the interatomic spacing in the Re islands is at least 10% larger than that of the Pt substrate. This is contrary to what is found in the bulk of single crystals, where the Re–Re nearest neighbor distance is approximately 0.5% shorter than the Pt–

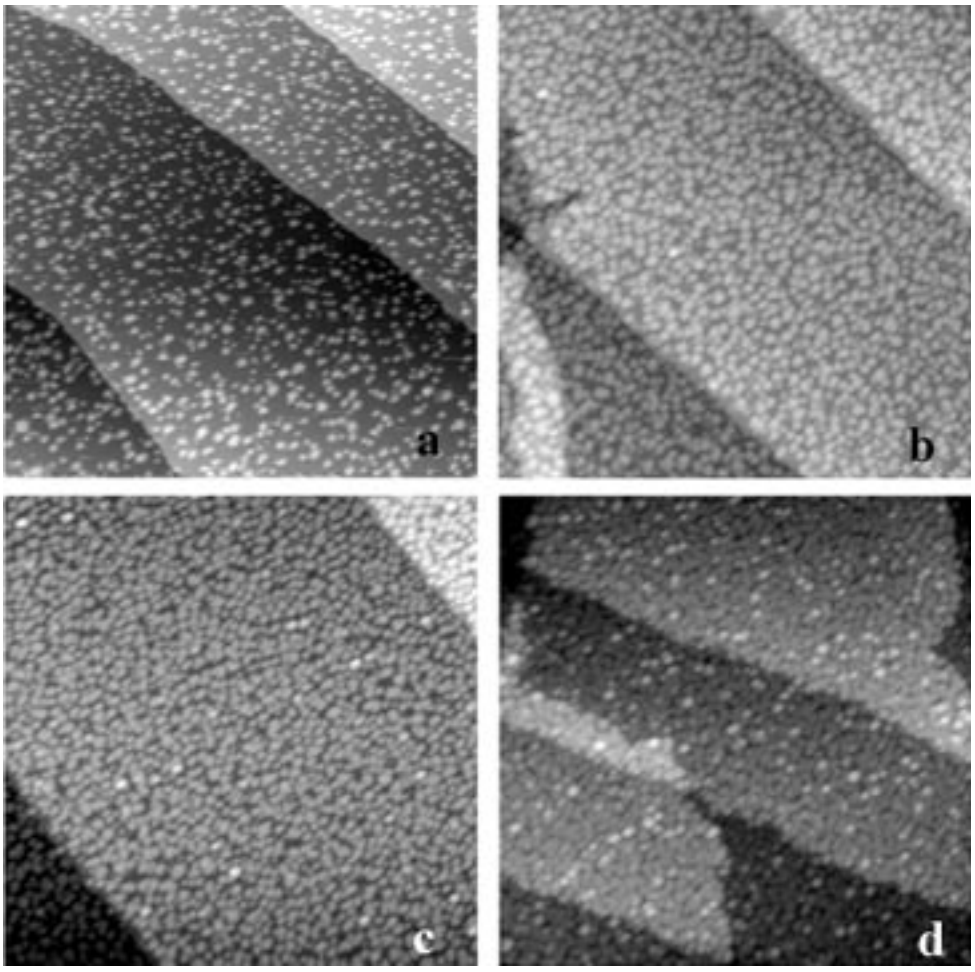

Fig. 1. 1000×1000 Å STM images of Re islands on Pt(111). The tip bias, tunneling current and Re coverage are as follows: (a) $U=0.07$ V and $I=4.27$ nA and $\theta=0.25$. (b) $U=0.35$ V and $I=4.91$ nA and $\theta=0.50$. (c) $U=0.52$ V and $I=6.65$ nA and $\theta=0.70$. (d) $U=0.52$ V and $I=8.38$ nA and $\theta=0.90$.

Pt distance. We observe the same Re–Re distance also for larger islands, but assume the possibility of compression in the Re overlayer once the islands start to coalesce. In Fig. 2, we also see that the perimeter of the island is imaged differently from the centre. In this case, the perimeter is blurred. In other cases, only the perimeter is imaged clearly. This is most likely a tip artifact, but could also be due to alloying around the edge of the island (see Section 3.2).

In order to calculate the amount of Re deposited in our photoemission experiments, we use the intensities of the $4f_{7/2}$ lines of Pt and Re. For a constant photon flux, these intensities may be written as:

$$I_{\text{overlayer}} = I^0_{\text{overlayer}}\theta(1-\alpha) \quad (1)$$

and

$$I_{\text{substrate}} = I^0_{\text{substrate}}[(1-\theta)+\alpha\theta], \quad (2)$$

where the Is denote Pt and Re $4f_{7/2}$ intensities, respectively, as indicated by the subscripts; overlayer = Re and substrate = Pt. The superscript '0' denotes the intensity from a clean single crystal of either Pt or Re, as given by the subscript ($I^0_{\text{overlayer}}$ is the intensity that would be measured

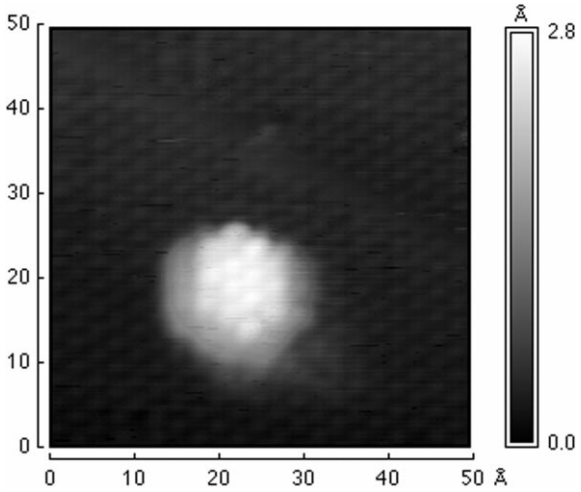

Fig. 2. Atomically resolved 50×50 Å STM image of a single Re island. The height is given by the grey scale, as indicated in the figure. $U = 0.01$ V and $I = 5.03$ nA.

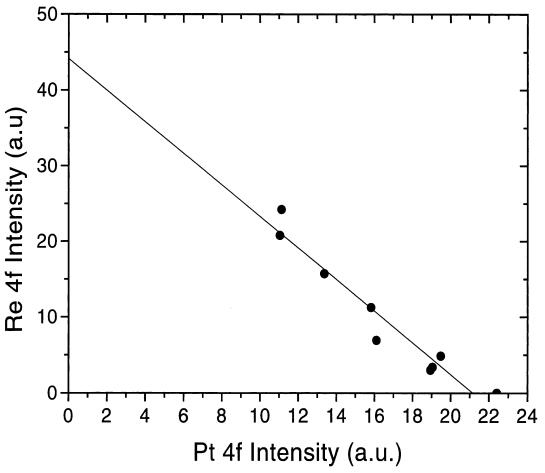

Fig. 3. Re 4f photoemission intensities plotted against the corresponding Pt 4f intensities. The line is a linear regression line. Its crossings of the axis define our choice of I^0_{Re} and I^0_{Pt} (see text for definitions). The intensities have been normalized with respect to the storage ring current.

from a Re crystal of the same morphology as our overlayers, and $I^0_{\mathrm{substrate}}$ is the intensity from the clean Pt(111) surface). θ is the overlayer (Re) coverage, and α is the fraction of emitted photoelectrons that pass through the overlayer without energy loss. α depends on the kinetic energy of the photoelectrons through their inelastic mean free path (IMFP); in a continuum model $\alpha = \exp(-d/\lambda)$, where d is the overlayer thickness and λ is the IMFP. We have used a photon energy of 130 eV for both Pt and Re $4f_{7/2}$, giving kinetic energies of ~ 50 and 90 eV, respectively. These kinetic energies both lie close to the broad minimum of the universal curve of IMFP [9]. We therefore choose the same value for α in Eqs. (1) and (2). If we were able to determine when, for instance, exactly 1 ML was deposited, we could find α experimentally. This is extremely difficult to do by vapour deposition. However, as we are able to distinguish surface and bulk emission from the clean Pt crystal, we can view the surface as the overlayer and the bulk as the substrate. Then, by setting $\theta = 1$ in Eq. (2), we find that α equals the bulk fraction of the Pt signal from clean Pt(111) ($I^0_{\mathrm{substrate}}$ is now the total emission, bulk and surface). This fraction is found to be approximately 0.45. Since the electronic mean free path is nearly element-independent, and we find that Re grows epitaxially on Pt(111) (a (1×1) LEED pattern is observed for thick Re layers by us and others [1,2]), we assume the same value of α also for the Re overlayer. For an overlayer thickness of 2.7 Å (the nearest neighbor distance in a Re single crystal) and an IMFP of 5 Å, we find $\alpha = \exp(-2.7/5) = 0.58$. Setting $\alpha = 0.5$ is thus a sound choice.

Combining Eqs. (1) and (2), we find that the two intensities should depend linearly on each other: $I_{\mathrm{Re}} = I^0_{\mathrm{Re}} + (I^0_{\mathrm{Re}}/I^0_{\mathrm{Pt}}) \cdot I_{\mathrm{Pt}}$ (here we have replaced the subscripts overlayer and substrate by Re and Pt, respectively). Fig. 3 shows that the experimental intensities indeed follow this linear behaviour. The plotted intensities have been normalized with respect to the storage ring current, which scales roughly linearly with the photon flux. Extrapolating to zero Pt intensity, we may read I^0_{Re} directly from the figure. We find $I^0_{\mathrm{Re}} = 44$ and $I^0_{\mathrm{Pt}} = 21$, and now have two formulae with which to decide the Re coverage, namely Eqs. (1) and (2). The most accurate results are obtained by combining Eqs. (1) and (2) and looking at the relative intensity . For each coverage, the Pt and Re 4f spectra are measured immediately after each other, ensuring only a small variation in the storage ring current. The assumption of linear scaling of

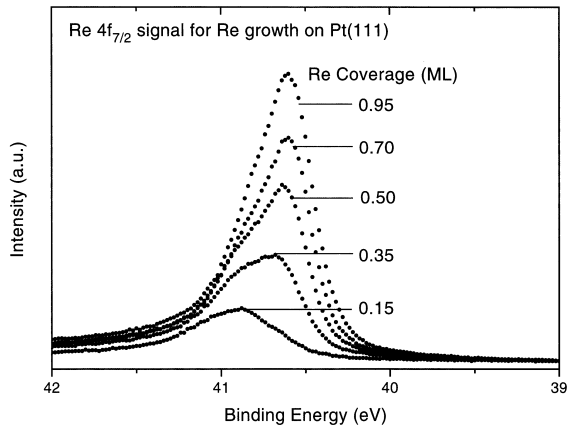

Fig. 4. Re $4f_{7/2}$ photoemission spectra for RT growth of Re on Pt(111). Re is deposited at RT. The sample is then cooled to 100 K and measured, then reheated to RT for new Re deposition, etc. The Re coverage for each spectrum, estimated as described in the text, is shown in the figure.

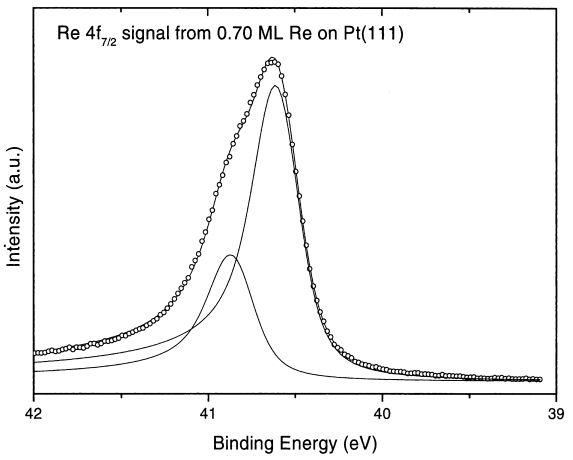

Fig. 5. Example of fit for Re $4f_{7/2}$ spectrum. The fitting functions are of DS type with Gaussian broadening and parameters as described in the text. The spectrum in the figure is obtained from a Re coverage of 0.70 ML. In this case, two components are required to fit the data, at binding energies of 40.60 and 40.80 eV respectively. For the lowest coverages, a third peak at 41.10 is also required.

the photon flux with the current should then be valid.

Fig. 4 shows Re $4f_{7/2}$ spectra for Re coverages ranging from 0.15 to 0.95 ML. The Re coverages have been estimated from the procedure described above and rounded to the nearest 0.05 ML. We estimate that the coverages thus defined are accurate to within ± 0.1 ML. Good fits of the spectra above 0.5 ML are obtained with two components at binding energies 40.60 and 40.80 eV, respectively, as shown in Fig. 5 for the case of a 0.70 ML Re coverage. A Doniach–Šunjić (DS) line shape [10], convoluted with a Gaussian distribution to account for phonon and instrumental broadening, is used to fit the spectra. A Lorentzian width (FWHM) of 0.16 eV, an asymmetry parameter of 0.15 and a Gaussian width (FWHM) of 0.20 eV were used. These parameters result from fitting a Re $4f_{7/2}$ spectrum containing a single peak (Section 3.2). For the lowest coverages, an additional component at 41.10 eV is required to fit the spectra. This component is due to residual Re alloyed in the surface region and is present before Re deposition (see the following section). We estimate that this amounts to less than 5% of the surface and it is soon buried during continued Re evaporation and becomes invisible. In the atomically resolved STM images of the 'clean' Pt(111) surface (not shown), we observe trimers of differently appearing atoms (lighter or darker, probably depending on the STM tip termination). We attribute these to the residual alloyed Re, either as trimers substituted in the surface layer, or as single Re atoms in the second layer. The STM images confirm that this amounts to less than 5% of the surface.

We also observe a slight (<0.1 eV) shift towards a lower binding energy for the Re $4f_{7/2}$ line as the coverage is increased (the major components at 40.65 and 40.88 eV for 0.15 ML to 40.57 and 40.79 eV just above 1 ML.). Based on variations in the quality of the fits as the binding energies are varied, we estimate that the uncertainty in the binding energies of the Re 4f components is less than 0.04 eV. Thus, the above-mentioned shifts are significant. We speculate that the origin of these small shifts is related to relaxation effects as the islands coalesce, forming long-range networks. One possible relaxation effect is a compression of the Re overlayer, as suggested above.

For a clean Re single crystal, the binding energy of the $4f_{7/2}$ electrons is 40.3 eV, and there is no resolved surface core-level shift (SCLS) associated with the (0001) surface [11]. For all Re overlayers

studied here, the $4f_{7/2}$ electrons have considerably higher binding energies than for bulk Re. The Re is thus perturbed by the contact with Pt. The absence of a SCLS for the Re(0001) surface suggests that replacing Re neighbors by 'vacuum-neighbors' only produces a small chemical shift for a Re atom. Since we now know that contact with Pt, however, produces a significant chemical shift, we argue that the two observed Re species differ mainly in their Pt coordination. From the STM images in Fig. 1, we see that second layer Re is only present for coverages very close to 1 ML, and even then never amounts to more than ~5% of the surface. Second-layer Re may therefore be ruled out as one of the two major components in the Re $4f_{7/2}$ signal. It may also be argued that this component is clearly not present in our spectra. In single-layer islands, there are also internal differences in Pt coordination; in the centre of the island, there is one Pt atom for every Re atom. On the edge of the island, there are fewer Re atoms to share each Pt atom; in other words, a higher Pt coordination. For Re adsorption in bridge sites, there is only one kind of edge atom (in addition to corner atoms, which are greatly outnumbered). Adsorption in threefold hollows sites, however, gives the possibility of having different edge coordinations. If the islands were triangular, all pointing in the same direction, there would be only one kind of edge atom. For hexagonal islands, there are two different edge coordinations and for more irregularly shaped islands, e.g. with ragged edges, the number of different Pt coordinations rapidly increases. Our STM images show hexagonal or more irregularly shaped islands (see Figs. 1 and 2). They do not allow us to discriminate between bridge or hollow site adsorption. If the Re chemical shift scaled approximately linearly with the Pt coordination, which is reasonable to a first approximation [12], our $4f_{7/2}$ spectra would be smeared out, not showing a clear shoulder (see Figs. 4 and 5), in the case of hollow site adsorption.

Another possibility is that the rather small differences in Pt coordination discussed above are not responsible for the shift seen in Figs. 4 and 5. Instead, it is possible that, already at RT, thermal processes equilibrate the edges of the islands to form an 'edge alloy', that is, an intermixed region around the islands. Alloy formation at island edges has been suggested for Pt on Re(0001), annealed to 1000 K [13], and is expected for Pt/Re(0001) and Re/Pt(111) due to negative surface mixing energies in both cases [14]. This model has the advantage of allowing a larger difference in the Pt coordination between the centre and the edges of the islands. A larger difference in coordination is also consistent with our discussion of chemical shifts as a function of Pt–Re coordination in the next section. Furthermore, if the edges are close to some metastable equilibrium, the local variation in coordination may be small. Alloying may also be responsible for the blurry appearance of the edges in STM (Fig. 2). Small variations around two well-separated coordination numbers fit well with having two contributions to the Re $4f_{7/2}$ line. To summarize: the component at approximately 40.6 eV originates from surface Re in the centre of the islands, whereas the component around 40.8 eV is associated with the island edges, possibly consisting of an alloyed region.

Decomposing the spectra of Fig. 4 in the manner shown in Fig. 5, we find that at 0.15 ML, the edge component dominates the spectrum. At 0.35 ML, the edge component is reduced to approximately 35% of the total Re 4f emission, and at still higher coverages, it is further reduced (23% at 0.95 ML). In comparison, a perfectly hexagonal island containing 91 atoms would have 30 atoms (33%) on the perimeter. This shows that the center-to-edge intensity ratio observed by photoemission is consistent with the STM results of Fig. 1,where we see well-separated islands containing ~100 atoms at the lower coverages. At higher coverages, we observe coalescence, reducing the number of edge atoms, but even at 90 ML, much of the island character is maintained.

The Pt $4f_{7/2}$ line for the same growth series (not shown, but see Fig. 8) is well represented by three peaks; two representing, respectively, bulk and surface Pt for the clean Pt(111) surface, and a third peak appearing as Re is deposited. DS functions have been used to fit the Pt spectra although, due to a sharp peak in the density of states of Pt at the Fermi level, this is not, strictly speaking, a good approximation (see Ref. [15] and references

therein). Still, the obtained fits have an acceptable quality, and we estimate a 0.1 eV accuracy in the resulting binding energies. We find, for the clean Pt(111) surface, bulk and surface components at 70.9 and 70.5 eV, respectively, in agreement with the literature ([16] and references therein). As Re is deposited, the surface component is attenuated, and a new component appears at 71.2 eV. This peak is considerably broader than that of the clean surface components, and shifts to 71.4 eV at the completion of the first ML.

3.2. Alloying by annealing

Annealing of the Re-covered surface produces rather dramatic changes in the Re 4f spectrum. Fig. 6 shows a series of such spectra recorded after annealing at increasing temperatures. First, a Re overlayer ($\theta=0.15$) is prepared at RT. The sample is then annealed for 1 min at each of the given temperatures. Measurements are taken between anneals, with the sample cooled to 100 K. After annealing to 1000 K, the Re $4f_{7/2}$ spectrum is reduced to a single, sharp peak which is well represented by a DS function. A lifetime broadening of 0.16 eV is found, in agreement with that

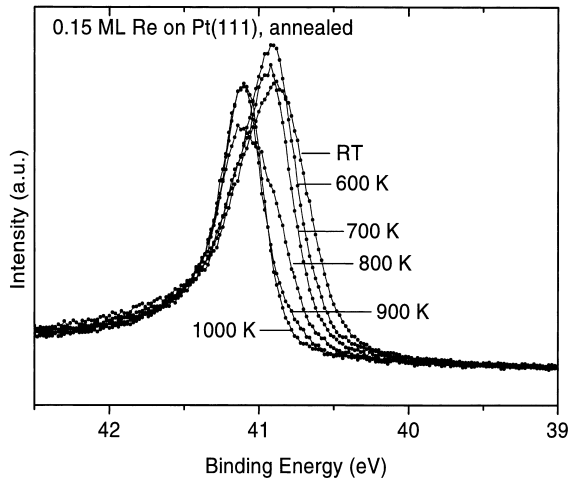

Fig. 6. Re $4f_{7/2}$ signal for a Re overlayer (0.15 ML) annealed at 600–1000 K, as indicated in the figure. The spectra are recorded with the sample at 100 K. The spectrum obtained after annealing to 1000 K is well represented by a single DS peak (at 41.98 eV).

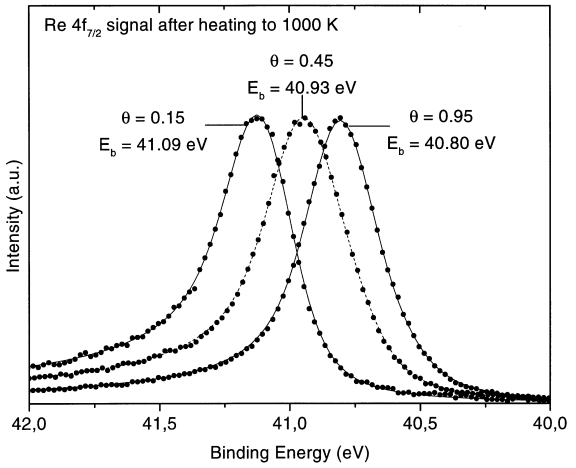

Fig. 7. Re $4f_{7/2}$ spectra recorded after annealing to 1000 K for three different initial Re coverages as indicated in the figure. The resulting binding energies are also shown. The lines show our fits to the data.

found for a Re single crystal [11]. A Gaussian broadening of 0.20 eV, which is reasonable for the present experimental resolution, is chosen. The position of the peak and its asymmetry parameter is found to decrease for increasing initial coverages (see Fig. 7). After annealing a $\theta=0.15$ overlayer to 1000 K, we measure a peak at $E_b=41.09$ eV with asymmetry $\alpha=0.20$, whereas a $\theta=0.95$ overlayer gives $E_b=40.80$ and $\alpha=0.11$. The corresponding values for bulk Re are $E_b=40.3$ and $\alpha=0.05$ [11]. As seen in the previous section, contact with Pt shifts the Re core levels towards higher binding energies. After annealing, a further shift is seen, indicating a higher Pt coordination for each Re atom. The increased asymmetry is also a sign of increased interaction with Pt. As the asymmetry is caused by low-energy electron hole pair excitations at the Fermi level, a change in asymmetry indicates a change in the Re density of states around E_f due to hybridization of Re and Pt 5d states. This could be accompanied by a Pt d→sp rehybridization, as discussed in Section 3.3.

Decomposing the spectra of Fig. 6 into three components, centre, edge, and alloyed Re, we may follow, in more detail, the development with temperature. As the temperature is increased, the centre component decreases monotonically. The edge component, however, increases in relative

intensity up to 700 K, whereas the alloy component is more or less unchanged. The most dramatic changes occur between 700 and 800 K; the alloy component grows and becomes dominant while the edge component declines. Heating to higher temperatures brings about a further reduction and growth of the edge and alloy components, respectively. At the same time, the alloy component is observed to shift from 41.14 eV at 800 K to 41.09 eV at 1000 K, indicating that the alloy becomes more Re-rich. The fact that the edge component gains intensity at the expense of the centre component for annealing temperatures up to 700 K, may be viewed as evidence that this state is itself an alloyed state, and that alloying proceeds from the periphery of the islands.

Fig. 8 shows the effect of Re deposition (0.15 ML) and subsequent heating on the Pt $4f_{7/2}$ spectrum. The most pronounced effect of heating

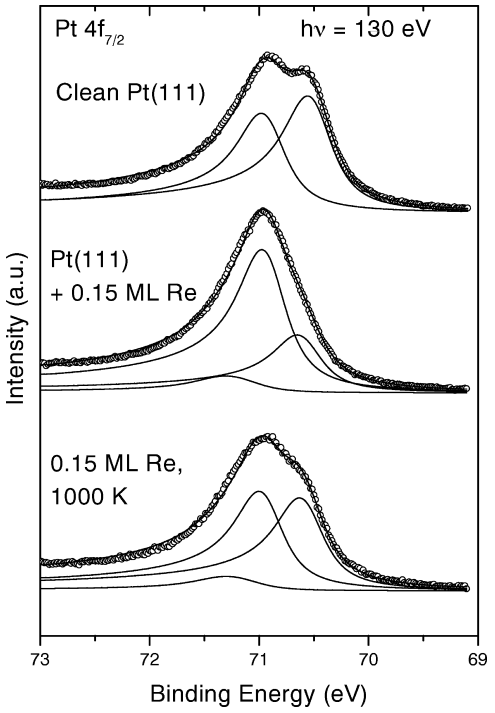

Fig. 8. Pt $4f_{7/2}$ signal for clean Pt(111) (upper spectrum), 0.15 ML Re on Pt(111) (middle), and the same surface after annealing to 1000 K (lower spectrum). All spectra are recorded at 100 K. Solid lines show our fits to the spectra containing the following components: Pt surface component at 70.5 eV, Pt bulk at 70.9 eV, and Pt in contact with Re at 71.2 eV.

to 1000 K is an increase in the surface component, showing that surface Re diffuses below the first Pt layer. This then makes more dilute solutions of Re in Pt possible, bringing each Re atom in contact with more Pt atoms. The increased asymmetry and binding energy for decreasing initial coverages seen for the Re $4f_{7/2}$ line in Fig. 7 fits well with this picture; less Re before heating leads to a more dilute alloy, resulting in a higher Pt interaction. In order to quantify this effect, we have estimated the Re concentration after annealing for several initial Re coverages. This is done by assuming that after annealing, the Re is evenly distributed among the n first layers (a reasonable assumption considering the sharpness of the corresponding Re 4f peaks, see above). The resulting changes in the intensities of Eqs. (1) and (2) are found by replacing the Re coverage θ by the concentration $c=\theta/n$, and α by α^n. By comparing with the experimental changes in intensity, we can determine n. For all the initial coverages, we find $n=3.0\pm0.3$. In Fig. 9, we have plotted the Re $4f_{7/2}$ binding energy as a function of the estimated Re concentration for the annealed surfaces. We have also included the case of single-layer Re on Pt(111) ($E_b=40.65$ eV), which corresponds to $c=0.5$ (i.e. a layered structure with every other layer Pt and Re) and bulk Re ($E_b=40.3$ [11]) corresponding to $c=1$. The linear regression line in the figure demonstrates that the binding energy scales linearly with the concentration over

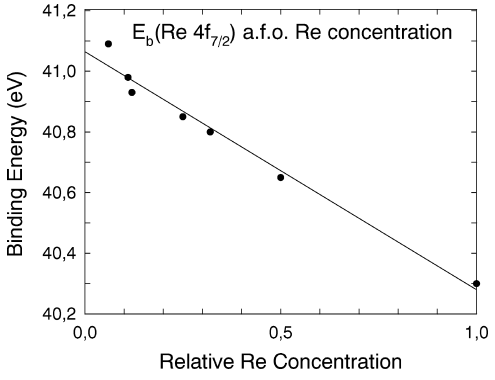

Fig. 9. Re $4f_{7/2}$ binding energy after annealing to 1000 K as a function of Re concentration (see text for estimation method). The 0.5 and 1.0 concentrations are 1 ML Re on top of Pt(111) and bulk Re (from Ref. [11]), respectively.

a surprisingly wide range of concentrations for the Re/Pt system.

We have seen that annealing at 1000 K produces a single Re $4f_{7/2}$ peak and that the position of this peak scales linearly with the Re concentration in the resulting alloy. To a first approximation, it is reasonable to assume that the chemical shift in an alloy depends only on the nearest-neighbor atoms. That is, each of the observed binding energies represents a given number of Pt nearest neighbors. As seen in Fig. 7, the separation between the different alloy peaks is well resolved. It is therefore clear that, for each concentration, one local coordination dominates completely. The Pt–Re phase diagram contains two regions with solid solutions; one Re-rich, the other Pt-rich with a maximum Re content of 40% [17]. Our Re concentrations after annealing are all in the latter region. Within this region there is an ordered Pt_3Re face with fcc structure [18]. As this is the only known ordered bulk structure for Re concentrations below 40%, there are three possible ways of describing the local order observed by photoemission:

1. solid solutions of Re in Pt have a high degree of local order,
2. the phase diagram is strongly modified by the presence of the surface and
3. we observe a series of structures that exist also in the bulk, but are metastable and therefore not previously observed.

Long-range order for each of the (more than five) concentrations observed is somewhat unlikely, and LEED always shows a (1×1) pattern after annealing. We therefore discard possibility (3). The influence of the surface seems evident from the fact that when order is reached, the Re is spread over three layers (not two or four), regardless of the initial coverage. Since we have not experimented with higher annealing temperatures or prolonged annealing, we cannot rule out the possibility that the observed states are metastable. In fact, a positive surface segregation energy has been calculated for Re/Pt(111) [14]. In conclusion, we have observed a series of alloy states with Re concentrations ranging from approximately 10 to 40%, all with a high degree of local order. The local order could be a feature of Re in Pt solid solutions, but could also be caused by the presence of the surface since the thermodynamics of the surface differ from that of the bulk (see, for example, Ref. [19]). A high degree of local order supports our assumption that the Re is evenly distributed in the three-layer region after annealing.

Returning now to the interpretation of the Re $4f_{7/2}$ component between 40.8 and 40.9 eV observed at RT, we have argued that this must be Re around the island edges, possibly alloyed with Pt. We can now use Fig. 9 to find approximately which Pt/Re coordination is responsible for this component. A value of 40.8 eV corresponds to a Pt/Re ratio of about 2, whereas for 40.9 eV, the ratio is close to 4. Even a ratio of 2 is high for an edge atom on top of the surface, giving further support for the existence of an intermixed region around the islands.

3.3. Valence band spectra

To gain insight into the details of the electronic interplay between Pt and Re, we have recorded valence band spectra for RT growth (Fig. 10) and alloying by annealing (Fig. 11). Fig. 10 shows the evolution of the valence band during Re growth.

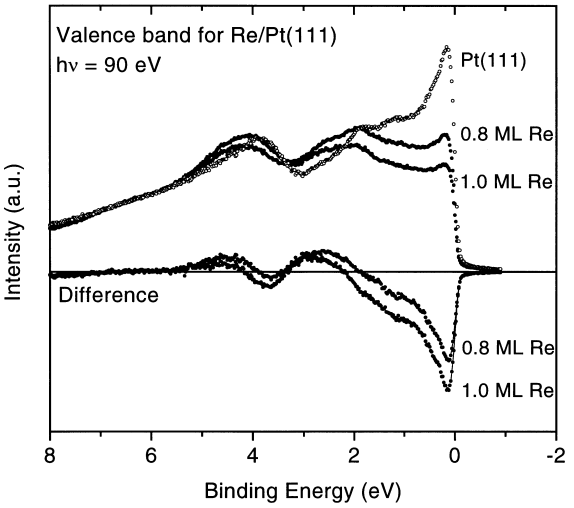

Fig. 10. Valence band spectra for RT growth of Re on Pt(111). Open symbols show the corresponding spectrum for clean Pt(111). The latter spectrum has been subtracted in the difference spectra in the lower part of the figure.

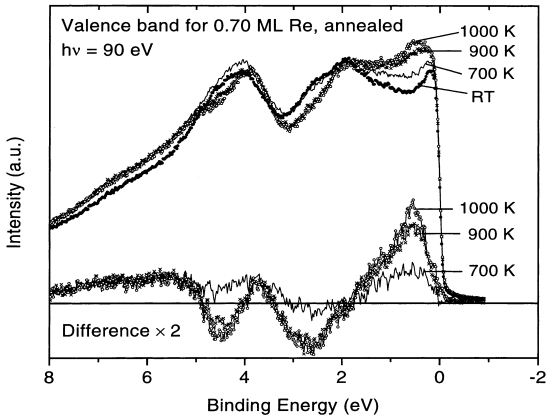

Fig. 11. Valence band spectra for a 0.70 ML Re overlayer annealed at 700–1000 K, as indicated in the figure. The spectra are recorded with the sample at 100 K. Difference spectra are obtained by subtracting the RT spectrum.

The most pronounced effect of Re adsorption is the strong attenuation of the sharp peak 0.2 eV from the Fermi edge in the Pt(111) spectrum. Clearly, this state is involved in the bonding to Re. The difference spectra of Fig. 10 reveal an increase in intensity around 2.6 eV as Re is deposited. This feature becomes quite prominent for thicker Re films (not shown), and is very likely a Re-derived state. We also note a reduction and increase in intensity at 3.7 and 4.5 eV, respectively, resulting from a shift towards higher binding energy of the Pt-derived feature around 4 eV.

Fig. 11 shows the development of the valence band spectrum as a 0.70 ML Re film is annealed. For annealing temperatures below 500 K, the spectrum is virtually unchanged. Higher temperatures result in an increased intensity around 0.6 eV. Both the clean and the Re-covered Pt(111) surface have states at 0.2 and 0.4 eV. Neither has a state at 0.6 eV; this is unique to the alloy. The Re-derived state at 2.6 eV is attenuated by annealing. This is explained by Re diffusing under the first Pt layer, as discussed in the previous section. The difference spectra in Fig. 11 also show features at 3.7 and 4.5 eV, but with opposite signs compared with Fig. 10; the feature around 4 eV shifts back towards a lower binding energy when the surface is annealed. A closer look at this feature reveals that it may consist of two independent peaks; its high- and low-energy sides vary independently with annealing temperature. Annealing temperatures up to 700 K result in a broad, positive feature in the difference spectrum around 3.8 eV. For higher temperatures, there is no change in intensity at this energy, but a sharp negative peak appears at 4.5 eV.

As seen in Fig. 10, there is a large depletion of Pt 5d states near the Fermi level when Re is deposited on Pt(111). Thus, the d-band centre of gravity shifts towards higher binding energy. This could be the cause of the positive core level shift for Pt in contact with Re [20,21]. A significant charge transfer between the two metals is unlikely [20,21] (and would most likely go from Re to Pt due to the difference in electronegativity). The most likely mechanism to explain the reduced Pt d density of states is a d→sp rehybridization of the Pt atoms in contact with Re. The sp valence states have a very low excitation cross-section. Thus, the gain in sp intensity is not observable in the present experiment. This type of d→sp rehybridization is common for group 10 metals in contact with sp or early transition metals [22].

When the Re overlayer is annealed, Fig. 11 shows an increase in Pt 5d intensity. This is only in part explained by the enrichment of Pt at the surface as the alloy is formed (this increase is larger than the decrease in Re intensity at 2.6 eV). As the alloy is formed, the Pt–Re coordination is changed so that the Re atoms are shared between a larger number of Pt atoms. This could mean that the perturbation of the Pt electronic structure becomes weaker, partly reversing the rehybridization described above.

4. Conclusions

We have studied the growth of Re in the submonolayer regime on the Pt(111) surface. By STM, it has been shown that the first Re layer grows as small (∼100 atom) islands. Less than 5% of second-layer atoms are observed when the first ML is nearly complete. High-resolution core-level spectroscopy has shown that there are two species of Re present on the island-covered surface at RT; atoms in the centre and around the edges of an

island. The edge Re species is in more intimate contact with Pt, i.e. very likely an 'edge alloy'. Annealing the Re-covered surface to 1000 K causes the formation of metastable surface alloys, extending over approximately three atomic layers. These alloys have a high degree of local order, with Pt/Re coordination depending on the Re concentration. Valence band spectra have shown a strong depletion of Pt 5d states near the Fermi energy when Re is adsorbed, possibly caused by a Pt d→sp rehybridization.

Acknowledgements

This work is financed, in part, by the Norwegian Research Council (NFR).

References

[1] F. Zaera, G.A. Somorjai, Surf. Sci. 154 (1985) 303.
[2] D.J. Godbey, G.A. Somorjai, Surf. Sci. 202 (1988) 204.
[3] D.J. Godbey, G.A. Somorjai, Surf. Sci. 204 (1988) 301.
[4] D.J. Godbey, F. Garin, G.A. Somorjai, J. Catal. 117 (1989) 144.
[5] C. Kim, G.A. Somorjai, J. Catal. 134 (1992) 179.
[6] W.T. Tysoe, F. Zaera, G.A. Somorjai, Surf. Sci. 200 (1988) 1.
[7] W. Unger, S. Baunack, Surf. Sci. 203 (1988) L682.
[8] J.N. Andersen, O. Björneholm, A. Sandell, R. Nyholm, J. Forsell, L. Thånell, A. Nilsson, Synchrotron Radiat. News 4 (1991) 15.
[9] D.R. Penn, Phys. Rev. B 13 (1976) 5248.
[10] S. Doniach, M. Šunjić, J. Phys. C 3 (1970) 285.
[11] N. Mårtensson, H.B. Saalfeld, H. Kuhlenbeck, M. Neumann, Phys. Rev. B 39 (1989) 8181.
[12] A. Nilsson, B. Eriksson, N. Mårtensson, J.N. Andersen, J. Onsgaard, Phys. Rev. B 38 (1988) 10357.
[13] M. Alnot, V. Gorodetskii, A. Cassuto, J.J. Ehrhardt, Thin Solid Films 151 (1987) 251.
[14] A. Christensen, A.V. Ruban, P. Stoltze, K.W. Jacobsen, H.L. Skriver, J.K. Nørskov, F. Besenbacher, Phys. Rev. B 56 (1997) 5822.
[15] G.K. Wertheim, L.R. Walker, J. Phys. F 6 (1976) 2297.
[16] O. Björneholm, A. Nilsson, H. Tillborg, P. Bennich, A. Sandell, B. Hernnäs, C. Puglia, N. Mårtensson, Surf. Sci. 315 (1994) L983.
[17] M. Hansen, Constitution of Binary Alloys, McGraw-Hill, London, 1958, and Suppl.
[18] L.I. Voronova, V.P. Polyakova, E.M. Savitskii, Izv. Akad. Nauk SSSR, Metally 1 (1984) 185.
[19] A. Zangwill, Physics at Surfaces, Cambridge University Press, Cambridge, 1988.
[20] M. Weinert, R.E. Watson, Phys. Rev. B 51 (1995) 17168.
[21] D. Hennig, M.V. Ganduglia-Pirovano, M. Scheffler, Phys. Rev. B 53 (1996) 10344.
[22] J.A. Rodriguez, Surf. Sci. 345 (1996) 347.